

Steady-State Nonequilibrium Density of States of Driven Strongly Correlated Lattice Models in Infinite Dimensions

A. V. Joura and J. K. Freericks

Department of Physics, Georgetown University, 37th and O Sts. NW, Washington, D.C. 20057, USA

Th. Pruschke

Institute for Theoretical Physics, University of Göttingen, Friedrich-Hund-Platz 1, D-37077 Göttingen, Germany
(Received 18 April 2008; revised manuscript received 6 October 2008; published 3 November 2008)

An exact formalism for calculating the retarded and advanced Green's functions of strongly correlated lattice models in a uniform electric field is derived within dynamical mean-field theory. To illustrate the method, we solve for the nonequilibrium density of states of the Hubbard model in both the metallic and Mott-insulating phases at half-filling (with an arbitrary strength electric field) by employing the approximate numerical renormalization group as the impurity solver. This general approach can be applied to any strongly correlated lattice model in the limit of large dimensions.

DOI: [10.1103/PhysRevLett.101.196401](https://doi.org/10.1103/PhysRevLett.101.196401)

PACS numbers: 71.27.+a, 71.10.Fd, 71.45.Gm, 72.20.Ht

Introduction.—The many-body formalism for nonequilibrium problems was formulated independently by Kadanoff and Baym [1] and Keldysh [2] in the 1960s. One of the main applications of that work was to determine the nonlinear transport properties of strongly correlated materials. Recently there has been a significant emphasis placed on examining small open systems (quantum dots attached to leads) within the Meir-Wingreen [3] generalization of the Kadanoff-Baym-Keldysh approach and there has been progress in applying Bethe ansatz [4] and numerical renormalization group techniques [5] within a scattering state formalism, and Hirsch-Fye quantum Monte Carlo techniques by mapping to an effective imaginary time formalism [6]. In this work, our focus is on larger systems (bulk materials) placed under large electric fields, which serves as a counterpart approach to the problem, and could have direct application to ultracold atomic systems placed in optical lattices that are driven into nonequilibrium by accelerating the lattice through space and measuring the density of states (DOS) [7].

There has also been much effort applied to understanding the original Kadanoff-Baym-Keldysh formalism. The generalized Kadanoff-Baym approximation [8] and the reconstruction theorem for the lesser Green's function [9] have provided much insight into the way quantum systems relax and ultimately reach a steady state. But there remains no exact solutions for strongly correlated bulk systems placed in large electric fields in the steady state. In this contribution, we move towards solving this problem by developing a nonperturbative technique to calculate the many-body DOS within the dynamical mean-field theory (DMFT) approach [10]. Since the retarded and advanced Green's functions are a needed input into the reconstruction theorem, this is an initial step toward a complete steady-state formalism. The development here is more general than the transient response formalism [11] because it can be applied to any many-body lattice Hamiltonian that

can be solved with a real time or real frequency impurity solver via DMFT; here we show results for the Hubbard model solved with the (approximate) numerical renormalization group (NRG).

Formalism.—Our focus is on the advanced and retarded Green's functions. Since the advanced Green's function is directly related to the retarded Green's function via complex conjugation and an interchange of the two time variables, we will derive results for the retarded Green's function only. We use the Keldysh boundary condition for the nonequilibrium problem: starting our system in an equilibrium distribution at a constant temperature and then turning on the constant and spatially uniform electric field. We then let the system evolve forward in time until all transients have died off and we are left with the steady-state response. The electric field is described by a spatially uniform vector potential in the Hamiltonian gauge, where the scalar potential vanishes $\mathbf{E}(t) = -\partial\mathbf{A}(t)/c\partial t$ and we ignore all magnetic field effects. For a uniform field, we then have $\mathbf{A}(t) = -c\mathbf{E}t$ since the field is turned on in the infinite past (but after the system has reached equilibrium at temperature $1/\beta$). The vector potential is input into the Hamiltonian via the Peierls' substitution [12], so that the nonequilibrium Hamiltonian is translationally invariant and can be described in momentum space; since current is flowing but the particle density is constant and we always project onto the lowest band in the lattice, the system acts as if it is attached to two reservoirs—one serving as a particle (or current) source and the other as a particle (or current) drain, allowing the steady state to emerge. The momentum-dependent retarded Green's function is defined to be

$$G_{\mathbf{k}\sigma}^R(t, t') = -i\theta(t - t')\text{Tr}e^{-\beta\mathcal{H}_{\text{eq}}}\{c_{\mathbf{k}\sigma}(t), c_{\mathbf{k}\sigma}^\dagger(t')\}_+ / Z_{\text{eq}}, \quad (1)$$

where the averages are taken with respect to the initial equilibrium Hamiltonian (Z_{eq} is the equilibrium partition

function), and the time evolution of the creation ($c_{\mathbf{k}\sigma}^\dagger$) and annihilation ($c_{\mathbf{k}\sigma}$) operators (for electrons with momentum \mathbf{k} and spin σ) is in the Heisenberg picture. We will examine the case where the electric field lies along the diagonal of a hypercubic lattice in d dimensions $\mathbf{E} = E(1, 1, 1, \dots)$ and then the limit where $d \rightarrow \infty$.

The retarded Green's function and self-energy Σ^R satisfy a Dyson equation that is formally equivalent to the equilibrium Dyson equation except that all functions now depend on two time variables instead of just the time difference

$$G_{\mathbf{k}\sigma}^R(t, t') = G_{\mathbf{k}\sigma}^{R0}(t, t') + \int d\bar{t} \int d\bar{t}' G_{\mathbf{k}\sigma}^{R0}(t, \bar{t}) \Sigma_{\sigma}^R(\bar{t}, \bar{t}') G_{\mathbf{k}\sigma}^R(\bar{t}', t'), \quad (2)$$

where the noninteracting steady-state Green's function can be found exactly [13,14]

$$G_{\mathbf{k}\sigma}^{R0}(t, t') = -i\theta(t-t') \exp\left[-i \int_{t'}^t d\bar{t} (\epsilon_{\mathbf{k}+E\bar{t}} - \mu)\right],$$

$$G_{\mathbf{k}\sigma}^{R0}(T, t_{\text{rel}}) = -i\theta(t_{\text{rel}}) e^{i\mu t_{\text{rel}}} \times \exp\left[-i \frac{2(\epsilon_{\mathbf{k}} \cos ET - \bar{\epsilon}_{\mathbf{k}} \sin ET)}{E} \sin \frac{Et_{\text{rel}}}{2}\right]. \quad (3)$$

Here, the band structure $\epsilon_{\mathbf{k}}$ satisfies [10] $\epsilon_{\mathbf{k}} = -\lim_{d \rightarrow \infty} t^* \sum_{i=1}^d \cos \mathbf{k}_i / \sqrt{d}$, the second band structure $\bar{\epsilon}_{\mathbf{k}}$ satisfies $\bar{\epsilon}_{\mathbf{k}} = -\lim_{d \rightarrow \infty} t^* \sum_{i=1}^d \sin \mathbf{k}_i / \sqrt{d}$ (all energies will be measured in units of t^* and we set $c = 1$), and the second line uses the Wigner coordinates of average time $T = (t + t')/2$ and relative time $t_{\text{rel}} = t - t'$. We will always work with the paramagnetic solution, so we drop the spin label on all functions.

The self-energy has no momentum dependence because we are working in the infinite-dimensional limit; the perturbative result of Metzner [15] and the Langreth rules [16] show that the self-energy is local in nonequilibrium as well. Note that the noninteracting steady-state Green's function satisfies the *gauge property* which relates shifts in momentum to shifts in average time

$$G_{\mathbf{k}+E\bar{t}}^{R0}(T, t_{\text{rel}}) = G_{\mathbf{k}}^{R0}(T + \bar{t}, t_{\text{rel}}), \quad (4)$$

where we write the Green's function as a function of the Wigner coordinates. It also satisfies the *Bloch periodicity property*, which shows the noninteracting system is periodic in the steady state

$$G_{\mathbf{k}}^{R0}(T + 2\pi/E, t_{\text{rel}}) = G_{\mathbf{k}}^{R0}(T, t_{\text{rel}}). \quad (5)$$

The gauge property implies that the local (summed over all momentum) noninteracting retarded Green's function is independent of average time, and the Bloch periodicity property implies that the momentum-dependent noninteracting retarded Green's function is periodic in average time with the Bloch period $2\pi/E$. The noninteracting lesser and

greater Green's functions are also periodic in the average time, with the Bloch period. Combining this with a perturbative expansion for the Green's functions or self-energies, immediately shows that both are also periodic functions with the Bloch period. We *define* the steady state as being the state where the retarded self-energy and local retarded Green's function are independent of average time, which is consistent with gauge-invariance arguments [17]. We next perform a continuous Fourier transformation with respect to relative time, and a discrete Fourier series expansion with respect to average time (with frequencies $\nu_n = nE$, integer multiples of the Bloch frequency) [$G_{\mathbf{k}}^R(T, t_{\text{rel}}) = \sum_n \int d\omega G_{\mathbf{k}}^R(\nu_n, \omega) \exp(-i\nu_n T - i\omega t_{\text{rel}})/2\pi$]. Then the Dyson equation in Eq. (2) becomes

$$G_{\mathbf{k}}^R(\nu_n, \omega) = G_{\mathbf{k}}^{R0}(\nu_n, \omega) + \sum_m G_{\mathbf{k}}^{R0}\left(\nu_m, \omega + \frac{1}{2}\nu_n - \frac{1}{2}\nu_m\right) \times \Sigma^R\left(\omega + \frac{1}{2}\nu_n - \nu_m\right) \times G_{\mathbf{k}}^R\left(\nu_n - \nu_m, \omega - \frac{1}{2}\nu_m\right), \quad (6)$$

which couples together the Green's functions at frequencies differing by multiples of the Bloch frequency; this equation has an underlying matrix structure to it that allows it to be solved in a straightforward fashion. In particular, we can restrict $0 \leq \omega < E$, and determine the Green's function at all $\omega + \nu_n$ (we became aware of a similar technique to solve the Dyson equation that employs Floquet matrices after this work was completed [17]). Summing over the momentum in the Brillouin zone produces the local Green's function, which is accomplished via a two-dimensional integration over the joint DOS $\rho(\epsilon, \bar{\epsilon}) = \exp(-\epsilon^2 - \bar{\epsilon}^2)/\pi$ [13].

The iterative DMFT algorithm [18] immediately applies to the nonequilibrium steady-state problem because the diagrammatic expansion for the local self-energy of the lattice, and for the self-energy of an impurity problem in an effective medium defined on the Keldysh contour are identical. Unfortunately, no general real-time impurity solver on the Keldysh contour has been developed yet, so we instead invoke the time-translation invariance of the retarded functions and Fourier transform the relative time to a frequency. Now a conventional solver in frequency space can be used, like the NRG impurity solver, but it requires us to use the steady-state density matrix for the impurity in weighting the expectation values for the Green's function. Since we do not know how to determine this density matrix without solving the full time evolution problem, we approximate the density matrix as a simple function of the impurity Hamiltonian, namely, the Boltzmann distribution $\exp(-\beta \mathcal{H}_{\text{imp}})$. It is difficult to quantify the errors that arise from this approximation, but the influence of the density matrix on the retarded Green's function is substantially smaller than on the lesser or greater Green's functions because the energy distribution

of the quantum many-body states should not depend on how those states are occupied. If the density matrix is just a function of the impurity Hamiltonian and can be determined independently, a simple modification of our NRG approach would then become an exact solution to the entire nonequilibrium problem. Nevertheless, the constant term in the self-energy and the first two moments of the imaginary part of the self-energy are exact within this approach [19], because they are determined solely by the filling of the electrons and the particle-hole symmetry; hence deviations can only enter at the second moment or higher. This approach is also known to be accurate when E is small [since corrections to the equilibrium DOS enter to $O(E^2)$], when U is small [since the distribution functions enter to $O(U^2)$ in the perturbative expansion for the self-energy], and when U is large at half-filling because the paramagnetic Mott insulator is well described by a Hubbard III approximation (where the distribution functions enter only via the particle densities which are explicitly conserved). All of the remaining nonequilibrium effects enter through the momentum-dependent Dyson equation and the self-consistency condition. Once the retarded Green's function is known, we compute the interacting DOS from $\rho(\omega) = -\text{Im}G_{\text{loc}}^R(\nu_n = 0, \omega)/\pi$. We verify the accuracy of this nonperturbative numerical solution by calculating the first three DOS moment sum rules [20] and the zeroth and first self-energy moment sum rule [19] (odd moments vanish at half-filling). In all cases considered here, the zeroth moment of the DOS satisfied the sum rule to 1% or better, the second moment had errors in the range from 1%–25%, while the zeroth moment of the self-energy had errors in the 15%–30% range. The accuracy for these moments is better than what is typically seen in exact equilibrium calculations, where errors for the second moment of the Green's function are often in the 40%–50% range (or higher) due to an overestimation of the bandwidth. All of this indicates that our approach is likely to be quite accurate for the nonequilibrium DOS in spite of the issues described above.

Results.—For concreteness, we solve for the nonequilibrium steady-state response of the Hubbard model [21] in infinite dimensions; the Hubbard model involves electrons hopping between nearest-neighbor sites, with an on-site repulsion U . The equilibrium Hamiltonian is

$$\mathcal{H}_{\text{eq}} = \sum_{\mathbf{k}\sigma} \epsilon_{\mathbf{k}} c_{\mathbf{k}\sigma}^\dagger c_{\mathbf{k}\sigma} + U \sum_{\mathbf{k}, \mathbf{q}, \mathbf{p}} c_{\mathbf{k}\uparrow}^\dagger c_{\mathbf{k}-\mathbf{q}\uparrow} c_{\mathbf{p}\downarrow}^\dagger c_{\mathbf{p}+\mathbf{q}\downarrow}, \quad (7)$$

and the nonequilibrium Hamiltonian results from the Peierls' substitution ($\epsilon_{\mathbf{k}} \rightarrow \epsilon_{\mathbf{k}+\mathbf{E}t}$ for the steady-state problem).

Details of the NRG algorithm appear in Ref. [22]. In most cases, we take $\Lambda = 1.6$ and keep 1600 states. We start by showing calculations for a weak field case, where $E = 0.5$ in Fig. 1. The four panels show progressively larger values of the interaction strength U ranging from metals (in equilibrium) to Mott insulators. In panel (a), we have the weak coupling result with $U = 0.5$. This behaves as ex-

pected, showing a broadening of the Wannier-Stark ladder delta functions [23], which are located at integer multiples of the Bloch frequency ($0.5n$ here). As the interactions increase further, the minibands broaden and merge into a single band, but with a shape unlike that seen in equilibrium [panel (b) for $U = 2$], and then they start to form the upper and lower Hubbard bands [panel (c) for $U = 4$ and panel (d) for $U = 8$]; note that in panel (c) there is still a small peak appearing at the center of the density of states. When comparing the Mott insulator results to those of the Falicov-Kimball model, where an exact solution is possible, the Mott-Hubbard bands of the Falicov-Kimball model are modulated at the Bloch frequencies and change their characteristic shape for dc fields; the upper and lower Mott-Hubbard bands do not show this behavior here, which could be a result of the approximate nature of the NRG impurity solver or could be a genuine difference between the two models (indeed for ac fields, the Falicov-Kimball model solution does not show such modulation [17]).

Note that the peak at low frequency should not be confused with the quasiparticle peak that appears in equilibrium. Indeed, the self-energy does not have a Fermi liquid form at all. The imaginary part does approach zero at $\omega = 0$ for small U , but it does not have a quadratic behavior in ω , and instead looks more like a cusp. When the interaction strength gets large enough, the self-energy develops a sharp peak at $\omega = 0$ reminiscent of the delta function peak for the Mott insulator in equilibrium.

In Fig. 2, we plot the nonequilibrium DOS for the strong field case of $E = 4$. Here the Bloch frequencies occur at

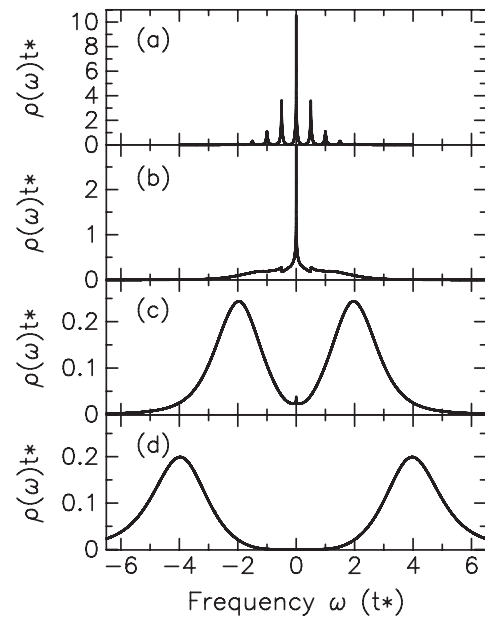


FIG. 1. Density of states for the infinite-dimensional Hubbard model with $E = 0.5$. The panels run from systems that are metallic to insulating (when in equilibrium): (a) $U = 0.5$; (b) $U = 2$; (c) $U = 4$; and (d) $U = 8$. Note the change in the vertical axis size for the different panels.

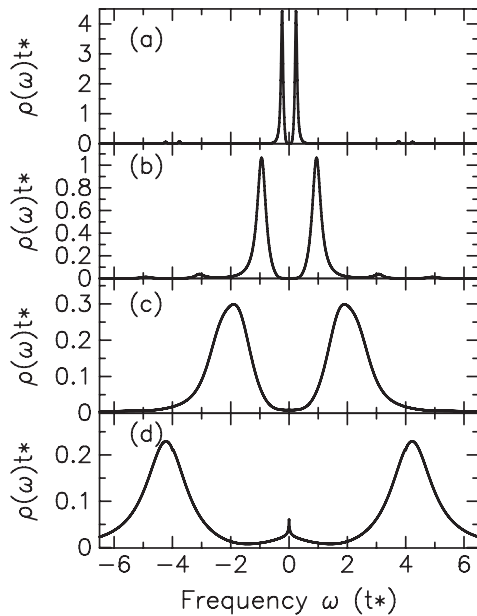


FIG. 2. Density of states for the infinite-dimensional Hubbard model with $E = 4$. The panels run from systems that are metallic to insulating (when in equilibrium): (a) $U = 0.5$; (b) $U = 2$; (c) $U = 4$; and (d) $U = 8$. Note the change in the vertical axis size for the different panels.

$4n$. For small U , the DOS corresponds to the Wannier-Stark ladder with the delta functions broadened but now also split by U [panel (a) with $U = 0.5$]; most of the spectral weight lies around $\omega = \pm U/2$, but there are still visible peaks around $\omega = \pm 4 \pm U/2$. When U is increased, the minibands also merge as in panel (b) for $U = 2$. One can see the splitting of the delta functions continues to increase, producing structure at $4n \pm 1$ now. In panel (c), we see a DOS for $U = 4$ that looks quite similar to the equilibrium DOS (but at a nonzero T). Panel (d) shows a new, and interesting effect. This case, with $U = 8$, has the delta functions (split by $\pm U/2$) that originate from the Wannier-Stark bands at $\omega = \pm 4$ “meeting” at $\omega = 0 = 4 - U/2 = -4 + U/2$, giving rise to the low-frequency peak in the DOS. The self-energy does not behave like a Fermi liquid here, though. Instead the self-energy has a three-peak structure for small U —two broad peaks centered near $\omega = \pm U$ and a narrow peak centered at $\omega = 0$. As U is increased, the broad self-energy peaks remain at $\omega \approx \pm U$, but the low-frequency peak disappears. Here, the self-energy looks like it is developing a power-law cusp at low frequency. The case with $U = 8$ is anomalous, with the shape of the DOS differing significantly from what is seen at $U = 6$ or $U = 10$, due to the anomaly of the meeting of the split Wannier-Stark peaks in the DOS.

Conclusions.—In this work, we have shown how to generalize DMFT to nonequilibrium steady-state situations and examined the many-body DOS for the Hubbard model driven by different magnitude electric fields. We find a rich array of behavior, including a broadening of the Wannier-Stark ladders, an evolution toward the equilibrium DOS

when U is large enough, and a splitting of the Wannier-Stark delta functions when E is large. The self-energy also is anomalous, and never appears to illustrate behavior similar to that of a Fermi liquid—the nonequilibrium steady state simply behaves differently.

We acknowledge useful conversations with F. Anders, A. Hewson, A.-P. Jauho, H.R. Krishnamurthy, V.S. Oudovenko, J. Serene, A.M. Shvaika, V.M. Turkowski, and V. Zlatić. A. V.J. and J.K.F. acknowledge support by the NSF under Grant No. DMR-0705266. Th. P. acknowledges support from the collaborative research center (SFB) 602.

- [1] L.P. Kadanoff and G. Baym, *Quantum Statistical Mechanics* (W.A. Benjamin, Inc., New York, 1962).
- [2] L. V. Keldysh, J. Exp. Theor. Phys. **47**, 1515 (1964) [Sov. Phys. JETP **20**, 1018 (1965)].
- [3] Y. Meir and N.S. Wingreen, Phys. Rev. Lett. **68**, 2512 (1992).
- [4] P. Mehta and N. Andrei, Phys. Rev. Lett. **96**, 216802 (2006).
- [5] F.B. Anders, arXiv:0802.0371.
- [6] J.E. Han and R.J. Heary, Phys. Rev. Lett. **99**, 236808 (2007).
- [7] M. Ben Dahan *et al.*, Phys. Rev. Lett. **76**, 4508 (1996); T.-L. Dao *et al.*, Phys. Rev. Lett. **98**, 240402 (2007); M. Fattori *et al.*, Phys. Rev. Lett. **100**, 080405 (2008).
- [8] P. Lipavský, V. Špička, and B. Velický, Phys. Rev. B **34**, 6933 (1986).
- [9] B. Velický, A. Kalvová, and V. Špička, J. Phys. Conf. Ser. **35**, 1 (2006).
- [10] W. Metzner and D. Vollhardt, Phys. Rev. Lett. **62**, 324 (1989); U. Brandt and C. Mielsch, Z. Phys. B **75**, 365 (1989).
- [11] J.K. Freericks, V.M. Turkowski, and V. Zlatić, Phys. Rev. Lett. **97**, 266408 (2006); J.K. Freericks, Phys. Rev. B **77**, 075109 (2008).
- [12] R.E. Peierls, Z. Phys. **80**, 763 (1933).
- [13] V.M. Turkowski and J.K. Freericks, Phys. Rev. B **71**, 085104 (2005).
- [14] V.M. Turkowski and J.K. Freericks, in *Strongly Correlated Systems: Coherence and Entanglement*, edited by J.M.P. Carmelo, J.M.B. Lopes dos Santos, V. Rocha Vieira, and P.D. Sacramento (World Scientific, Singapore, 2007), p. 187.
- [15] W. Metzner, Phys. Rev. B **43**, 8549 (1991).
- [16] D.C. Langreth, in *Linear and Nonlinear Electron Transport in Solids*, edited by J.T. Devreese and V.E. van Doren (Plenum Press, New York and London, 1976), p. 3.
- [17] N. Tsuji, T. Oka, and H. Aoki, arXiv:0808.0379.
- [18] M. Jarrell, Phys. Rev. Lett. **69**, 168 (1992).
- [19] V.M. Turkowski and J.K. Freericks, Phys. Rev. B **77**, 205102 (2008).
- [20] V.M. Turkowski and J.K. Freericks, Phys. Rev. B **73**, 075108 (2006); Phys. Rev. B **73**, 209902(E) (2006).
- [21] J. Hubbard, Proc. R. Soc. A **276**, 238 (1963).
- [22] R. Bulla, Th. A. Costi, and Th. Pruschke, Rev. Mod. Phys. **80**, 395 (2008).
- [23] G.H. Wannier, Phys. Rev. **117**, 432 (1960).